Inhibition of Single *Shaker* K Channels by κ−Conotoxin-PVIIA

David Naranjo

Instituto de Fisiología Celular, Universidad Nacional Autónoma de México, Circuito Exterior, Ciudad Universitaria,
04510 México DF, México

ABSTRACT   κ−Conotoxin-PVIIA (κ−PVIIA) is a 27-residue basic (+4) peptide from the venom of the predator snail *Conus purpurascen*s. A single κ−PVIIA molecule interrupts ion conduction by binding to the external mouth of *Shaker* K channels. The blockade of *Shaker* by κ-PVIIA was studied at the single channel level in membrane patches from *Xenopus* oocytes. The amplitudes of blocked and closed events were undistinguishable, suggesting that the toxin interrupts ion conduction completely. Between −20 and 40 mV κ-PVIIA increased the latency to the first opening by one order of magnitude in a concentration-independent fashion. Because κ-PVIIA has higher affinity for the closed channels at high enough concentration to block >90% of the resting channels, the dissociation rate could be estimated from the analysis of the first latency. At 0 mV, the dissociation rate was 20 s^{-1} and had an effective valence of 0.64. The apparent closing rate increased linearly with [κ-PVIIA] indicating an association rate of 56 μM^{-1} s^{-1}. The toxin did not modify the fraction of null traces. This result suggests that the structural rearrangements in the external mouth contributing to the slow inactivation preserve the main geometrical features of the toxin-receptor interaction.

INTRODUCTION

κ−Conotoxin-PVIIA (κ−PVIIA) is a marine snail toxin that has converged with α−Ktx scorpion toxins to a common mechanism of inhibition of K channels. These toxins occlude the external entrance of the most conserved functional locus of these membrane proteins, the ion conduction pore (MacKinnon and Miller, 1988; Goldstein and Miller, 1993; García et al., 1999). Both types of toxins, although distantly related, share important structural features: they are short, structurally constrained peptides having three intramolecular disulfide bonds (Bontems et al., 1992; Scanlon et al., 1997; Savarin et al., 1998). As several other K-channel specific peptides, the residues involved in the molecular recognition of their receptor, usually basic and hydrophobic, are proposed to be located on the same face of the peptide (Stampe et al., 1994; Goldstein et al., 1994; Jacobsen et al., 2000; Dauplais et al., 1997).

The dissociation rate of the toxin-channel complex is sensitive to the internal concentration of permeant ions and to the electric field across the membrane. For α−Ktx, this characteristic disappeared when neutral Asn or Gln substituted a conserved Lys at position 27. These results suggested that during the binding event by α−Ktx, the side chain of Lys-27 is exposed to the pore, making close range electrostatic repulsion with the permeant cations residing in the conduction pathway (Park and Miller, 1992; Goldstein and Miller, 1993). For κ−PVIIA, mechanistic conclusions similar to those of the α−Ktx family were reached.

κ−PVIIA compete with tetraethylammonium (TEA), a well-known K-channel pore blocker, and is stabilized when internal permeant ions are removed (García et al., 1999).

Such conclusions were based on the analysis of macroscopic currents, assuming 1) the toxin binding is a discrete event of occlusion of the K-channel pore, and 2) the channel-toxin complex is nonconductive. The κ−PVIIA blockade of *Shaker* K-channel using single channel recordings was examined. Analysis at this observation level supports the basic assumptions. κ−PVIIA binds in a concentration-dependent but voltage-independent manner. The toxin unbinding is voltage-dependent and concentration independent. Interestingly, κ−PVIIA does not modify the fraction of null traces, or the rate of macroscopic slow inactivation, a process involving a structural rearrangement of the toxin receptor (for example, see López-Barneo et al., 1993; Yellen et al., 1994; Larsson and Elinder, 2000). Similar results have also been found with α−Ktx (Liu et al., 1996), suggesting that those structural rearrangements must preserve the main geometrical features of the toxin receptor.

MATERIALS AND METHODS

Salts of analytical grade were purchased from Baker, México. *N*-methyl-D-glucamine, gentamicin, EGTA, HEPES, and bovine serum albumin were from Sigma (Sigma-Aldrich, Química S.A. de C.V., México). Type II collagenase was from Worthington Biochemical Corporation (Freehold, NJ). κ−Contoxin-PVIIA was a gift from Dr. Martin Scanlon (3D Center, University of Queensland, St. Lucia, Australia). *Xenopus* laevis females were from *Xenopus* One (Dexter, MI).

Heterologous expression of *Shaker* K channels

Shaker BΔ(6−46), dubbed here *Shaker* (Hoshi et al., 1990), was subcloned in pBluescript KS. After surgically removed, oocytes were treated with collagenase type II in ND96 solution: 96 mM NaCl, 2 mM

KCl, 1.8 mM CaCl$_2$, 1 mM MgCl$_2$, 10 mM HEPES, pH 7.6, and 50 μg/mL gentamicin. Stage IV-VI oocytes were isolated and manually defolliculated in a nominally Ca^{2+}-free ND96 solution. Oocytes were injected with 0.05 to 0.2 ng of cRNA obtained from in vitro translation (message Machine, Ambion Inc., Austin, Texas). After injection, they were incubated at 18°C in ND96 supplemented with sodium pyruvate (2.5 mM) and bovine serum albumin (0.04%). After 15- to 72-h incubation, subsequent patch clamp recordings were made at room temperature (22°C–24°C).

Electrophysiology

Patch pipettes for outside out recording (1–4 MΩ) were filled with two types of internal solutions: *100-K* consisted of: 80 mM potassium fluoride, 20 mM KCl, 1 mM MgCl$_2$, 10 mM EGTA, and 10 mM HEPES-KOH, pH 7.4 and *15-K* consisted of 90 mM *N*-methyl-D-glucamine fluoride, 10 mM KF, 1 mM MgCl$_2$, 10 mM EGTA, and 10 mM HEPES-KOH, pH 7.4. The external recording solution was 115 mM NaCl, 1 mM KCl, 0.2 mM CaCl$_2$, 1 mM MgCl$_2$, and 10 mM HEPES-NaOH, pH 7.4. From a holding voltage of −90 mV, 200-ms voltage pulses were applied every 5 s for macroscopic currents, and every second to promote appearance of null traces in the single channel recordings. An Axopatch 1D amplifier, complemented with a HIS-1 integrating headstage, was used for recording (Axon Instruments, Foster City, CA). The signal was online filtered to 500 Hz with an 8-pole Bessel filter 900 (Frequency Devices, Haverhill, MA), and acquired with an Axon Digidata 1200B interface at a sampling interval of 250 μs. Individual *Shaker* K channels in patches had a tendency to stop functioning, and 50% of the 16 single channel recordings used here ended because of the disappearance of channel activity. All analyses were from recordings starting with a single channel or due to K-channel disappearance ended with a single channel. A patch was considered having a single channel when, after 10 consecutive pulses, no signs of simultaneous openings were seen. The probability of not seeing a double opening in *n* consecutive trials if there were at least two channels would be $< [2p_o(1 - p_o)]^n$, where p_o is the channel open probability. For example, within the first 10 ms at +40 mV, the overall single *Shaker* open probability (including null traces) in the absence of κ−PVIIA, p_o, was 0.6 to 0.9. At the tenth consecutive trial, the probability of not seeing a double opening in a two-channel patch should be <0.00065 (Naranjo and Brehm, 1993).
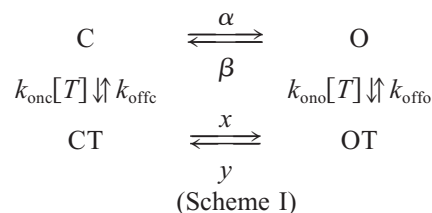
To compare directly the effects of different toxin concentrations on the same membrane patch, measurements were made in the outside-out configuration. Single channel recordings were acquired in blocks of 30 traces. Each recording started with a block of control traces to ensure a comparison between toxin and at least one block of controls. Here is defined an experiment as a measurement with toxin that had at least a block of 30 control traces to compare data from the same patch.

Data analysis

Single channel analysis was made with pClamp 5.5 software suite (Axon Instruments). Before event analysis, a minimum of four of the nearest nulls traces were averaged and subtracted each record. After ignoring the first 2 ms into the voltage pulse, threshold for event detection was set to 50% amplitude, and event durations were measured in multiples of 250 μs. Detection threshold was at least 2.5 times the SD of the baseline noise. No correction was made for missing events. Curve fitting, statistics, and figure preparation were carried out with Microcal Origin 3.5 and 4.1 (Microcal Inc, Northampton, MA).

Kinetic analysis and simulations

Both open and closed conformations of the *Shaker* K-channel are competent to bind κ−PVIIA with a bimolecular stoichiometry according to the following oversimplified scheme (Terlau et al., 1999).

$$C \underset{\beta}{\overset{\alpha}{\rightleftarrows}} O$$

$$k_{onc}[T] \Updownarrow k_{offc} \qquad k_{ono}[T] \Updownarrow k_{offo}$$

$$CT \underset{y}{\overset{x}{\rightleftarrows}} OT$$

(Scheme I)

in which [T] is the toxin concentration, C, O, CT, and OT correspond to the unblocked-closed, unblocked-open, blocked-closed, and blocked-open channels, respectively. The constants k_{ono}, k_{onc}, k_{offo}, and k_{offc} correspond to the association rates to the open and closed channels and to the dissociation rates from the open and closed channels, respectively. Rates α and β are, respectively, for opening and closing of the unblocked channel, whereas x and y are the corresponding rates for the blocked channel. For each experimental condition, 10^5 events were simulated with an in-house FORTRAN program according to DeFelice and Clay (1983). All rate constants, except for x and y, can be measured experimentally, so I assumed microscopic reversibility in the form of: $y/x = (\beta \times k_{onc} \times k_{offo})/(\alpha \times k_{ono} \times k_{offc})$. As long as the ratio y/x was maintained constant, giving values from 0.01 to 10 ms^{-1} to rate x did not introduce obvious modifications to the open and shut times distributions. Events briefer than the theoretical dead time of a 500-Hz Gaussian filter (360 μs) were ignored (Colquhoun and Sigworth, 1983). Cumulative and probability density function distributions were calculated for one or two exponential components, and the negative logarithm of the likelihood was maximized with a Gauss-Newton algorithm (Alvarez et al., 1992).

RESULTS

κ−Conotoxin-PVIIA is a peptide toxin that blocks open *Shaker* K-channel with a 1:1 stoichiometry in a voltage-dependent fashion. Under physiological ionic conditions, κ-PVIIA exhibits one order of magnitude higher affinity for the closed than for the open state; thus, the same voltage pulse used to open the voltage gated *Shaker* K-channel also destabilize the toxin-channel complex (Scanlon et al., 1997; García et al., 1999; Terlau et al., 1999). Fig. 1 summarizes the toxin effect on the N-inactivation removed *Shaker* Δ(6− 46), in a typical outside-out macropatch experiment. In comparison with its control (Fig. 1 *A*), the most prominent effects of continuous application of 500 nM κ-PVIIA are the current reduction and a slowed activation kinetics (Fig. 1 *B*). To analyze this time-dependent effects, for voltages pulse positive to −20 mV the κ-PVIIA traces were divided point-by-point by their respective control traces (Fig. 1 *C*). These quotient traces represent normalized time-courses of the toxin destabilization at each voltage (Scanlon et al., 1997). They are consistent with relaxations to voltage-dependent, lower-affinity equilibriums.

When 85% of the intracellular potassium was replaced with *N*-methyl-D-glucamine, the time-dependent decrease of the current in the control traces became more pronounced (Fig. 1 *D*). At the end of a 200-ms voltage pulse to 50 mV
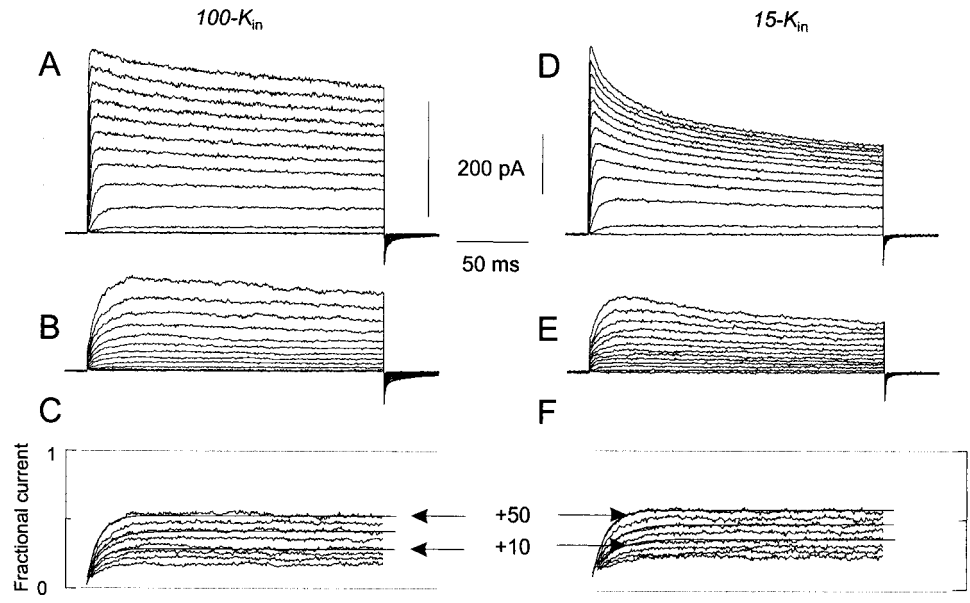
FIGURE 1 Macroscopic inhibition of K currents by κ−PVIIA in outside-out membrane patches. Left and right panels correspond to outside-out macropatch traces obtained with 100 and 15 mM K$^+$ in the pipette. Traces in the absence (*A* and *D*) and presence (*B* and *E*) of 0.5 μM κ−PVIIA. (*C* and *F*) Point-by-point division of records in the presence of the toxin by their respective control records at voltages positive to −20 mV. Lines on top of some traces are single exponential fits extrapolated to the beginning of the voltage pulse to estimate an average resting inhibition (only shown +10, +30, and +50 mV for clarity).

the average current reduction was 45 ± 6% (*n* = 18) compared with 23 ± 6% (*n* = 30) seen in normal high internal potassium (mean ± SD). Consistent with C inactivation, this time-dependent decrease was nearly voltage independent between −10 and +60 mV (not shown; Hoshi et al., 1991; Marom and Levitan, 1994).

At this low internal potassium, 500 nM κ-PVIIA also introduced the apparent delayed activation seen previously (Fig. 1 *E*). The quotient traces (Fig. 1 *F*) show very similar time-courses of the toxin destabilization to those seen in normal high internal potassium. From single exponential fits to each quotient relaxation in Fig. 1, *C* and *F*, time constants and steady-state inhibitions were obtained at each voltage.

From these values, assuming a simple 1:1 stoichiometry, the rates of toxin binding and unbinding to the open channels, k_{ono} and k_{offo} respectively, were obtained at the two internal potassium concentrations (García et al., 1999; see

Table 1). The similarity of the constants between 15 and 100 mM internal potassium indicates that in this concentration interval the toxin is little although significantly dependent on the internal potassium concentration. Moreover, the horizontal asymptotes of the quotient relaxations suggest that the slow inactivation is unaffected by the toxin presence (see Discussion).

Single channel recordings

Proposed blockade and docking mechanisms assume that κ-PVIIA binding to the external vestibule is a discrete event that results in the complete occlusion of the K-channel permeation pathway (García et al., 1999; Terlau et al., 1999; Jacobsen et al., 2000). However, the very shallow dependence on internal potassium seen in the experiments of Fig. 1 may suggest that the toxin binding is not in intimate

TABLE 1   Summary of the kinetic parameters of κ-PVIIA blockade on *Shaker*-IR

Experimental condition	k_{ono} (μM^{-1} s^{-1})	$z\delta_{ono}$	k_{offo} (s^{-1})	$z\delta_{offo}$	K_{Do} (μM)	Observation
Macropatch						
K_{in}−100/K_{out}−1	52 ± 4	0.03 ± 0.04	25 ± 3	0.64 ± 0.06	0.48 ± 0.06	García et al., 1999
K_{in}−15/K_{out}−1	32 ± 2	0.14 ± 0.07	10 ± 1	0.47 ± 0.08	0.31 ± 0.04	García et al., 1999
Single channel	56 ± 8	−0.05 ± 0.15	20 ± 8	0.64 ± 0.09	0.36 ± 0.07	This work

For single channel data k_{ono} and k_{offo} were measured from the equation in legend to Fig. 4 and from the first latency measurements, respectively. K_{Do} was obtained from k_{offo}/k_{ono}.
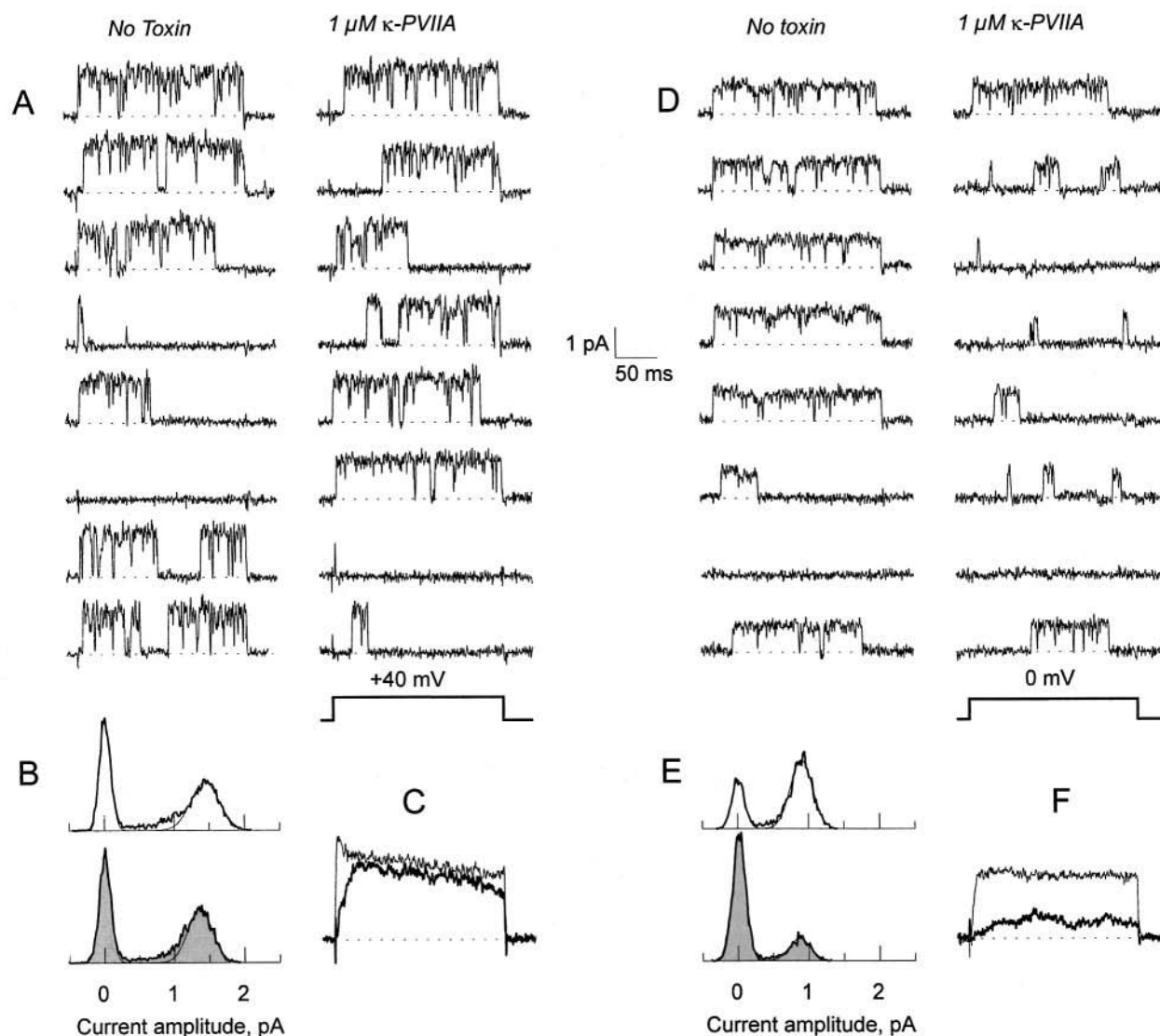
FIGURE 2   κ−PVIIA inhibition of *Shaker* K channels at microscopic level. Single channel recordings at +40 (*A*) and 0 mV (*D*) in the presence and in the absence of 1 μM κ−PVIIA. Channel openings were elicited by 200-ms pulses every 1 s to maximize the frequency of null traces. Traces were low-pass filtered with an 8-pole Bessel filter to 500 Hz, sampled at 4 kHz. Records shown were obtained after subtraction of 5 to 10 averaged null traces. For display, some traces outside the pulse zone were baseline corrected. Dashed lines indicate the zero-current level. (*B* and *E*) All points amplitude histogram in control and with 1 μM κ−PVIIA (*open* and *filled histograms*, respectively). Continuous lines in the histograms are Gaussian fits to the closed and open amplitudes. For +40 mV, current amplitudes for control and in toxin are 1.41 ± 0.46 and 1.35 ± 0.34 pA, respectively. For 0 mV, current amplitudes for control and in toxin are 0.90 ± 0.3 and 0.87 ± 0.3 pA, respectively. *C* and *F* correspond to ensemble averages of currents of 20 control traces (*thin lines*) and with toxin (*thick lines*). Quantitatively, the levels of inhibition resulting from these two ensembles of such small number of traces do not agree with those of the macroscopic currents. At +40 mV, the inhibition appears to be underestimated, and at 0 mV, it appears to be overestimated. However, qualitatively these ensembles show the basic macroscopic behavior of the *Shaker* K channels in the toxin presence, an apparent slower activation due to an increased first latency.

contact with the pore, which is a situation that could give rise to an incomplete pore occlusion, as δ−dendrotoxin blocks this channel (Imredy and MacKinnon, 2000). To my knowledge, there is no single channel study of the action of κ-PVIIA on *Shaker* K channels to validate those early assumptions. Single channel recordings were performed to study the interaction of the κ-PVIIA with *Shaker* K-channel at the microscopic levels. Figs. 2 to 4 deal with the mech-

anistic aspects of the κ-PVIIA inhibition on open *Shaker* K channels.

Fig. 2 shows leak and capacitance subtracted single channel traces from the same outside-out membrane patch responding to 200-ms pulses to +40 (A) and 0 mV (D). Each panel presents eight consecutive traces in control and with 1 μM κ-PVIIA. Except for an increased latency to the first opening in the presence of the toxin at +40 mV, the
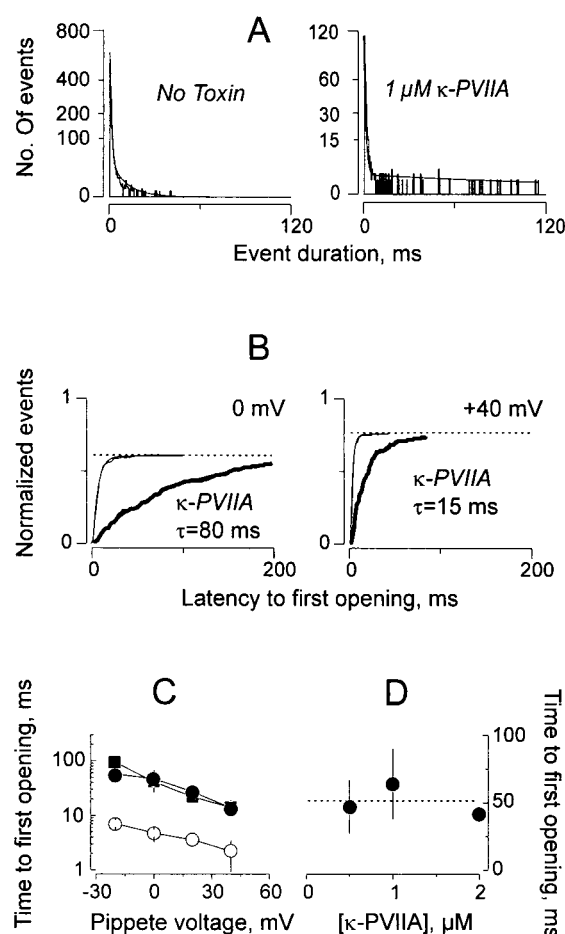
FIGURE 3 Dissociation rate constant of κ−PVIIA. (*A*) Shut distributions in control (*left panel*) and in the presence of 1 μM κ−PVIIA for the experiment shown in Fig. 2 at 0 mV (*right panel*). Amplitude of the distributions is shown as square root to emphasize the low frequency of longer blocked events. Solid lines are two-exponential fits to the distributions as follows: control, 0.83 ms (88% of the events) and 5.3 ms; with 1 μM κ−PVIIA, 0.84 ms (54% of the events) and 81 ms. (*B*) The toxin increased the latency to the first opening, suggesting that this measure corresponds to the unbinding of the toxin (see text). Analysis of the experiments from Fig. 2, at 0 and +40 mV, reveals that with 1 μM κ−PVIIA the first latency is increased by a factor of 5 to 20. Thin lines are the first latency distribution in the absence of the toxin, whereas thick lines are the distribution of the first latencies in the presence of the toxin. All distributions were made ignoring the first 2 ms into the voltage pulse. Single exponential fits are plotted on top of each distribution, and the obtained time constants are shown for 0 and +40 m. Note that the asymptotic values in each condition are not toxin dependent (*dotted lines*). (*C*) Effect of κ−PVIIA and voltage on the first latency. In comparison to the control (○), κ−PVIIA at 0.5 μM (●) or 2 μM (■) increased equally the first latency by a factor of 10. The first latency was obtained from the exponential fits to distributions as those shown in *B*. In the presence of the toxin at 0 mV the first latency was 45 ± 6 ms with an effective valence of 0.64 ± 0.22 (±SD; n = 7 patches). (*D*) Average values of the first latency measured experimentally at 0 mV. Plotted values correspond to averages (±SD) of 3, 4, and 2 patches for 0.5, 1, and 2 μM of κ−PVIIA, respectively. Dotted line is the weighted average.

differences from the control traces are subtle (Fig. 2 *A*). However, with the voltage pulse to 0 mV, the differences are more obvious (Fig. 2 *D*). The first detected opening occurs later in the record, and the nonconducting events are prominently longer than in the control. Ensemble average of 20 traces such as those of A and D, with and without toxin, are shown in thick and thin traces, respectively, in Fig. 2, *C* and *F*. Such ensemble averages qualitatively agree with the records shown in Fig. 1. Thus, the increased latency to the first opening seems to be responsible for the apparently retarded activation kinetics seen in macroscopic recording.

No significant differences in the single channel conductance were detected when amplitude histograms with (shaded) and without toxin (nonshaded) were compared (Fig. 2, *B* and *E*). Additional measurements with the two-electrode voltage clamp in the presence of 50 μM toxin in whole oocytes left a residual current of 5 ± 2% (n = 2). Without making bold assumptions about the behavior of leakage in this experimental condition, such a small residual could not be distinguished from endogenous outward currents (not shown). Thus, if the toxin does not occlude completely the conduction pathway, the residual current is below detection level.

To evaluate the kinetics of κ−PVIIA on the single *Shaker* K channel behavior, open and shut time distributions were constructed using the half amplitude threshold. The analysis of the traces taken at 0 mV of the patch shown in Fig. 2 were chosen as representative results to illustrate effect of the toxin on the shut and open distributions (Fig. 3 *A* and 4 *A*, respectively). In the following paragraphs, the rationale to obtain the toxin's association and dissociation rate constants from this analysis are described.

Shut time distribution and the dissociation rate constant

In general, two exponential components fitted well the shut duration distributions in control conditions and with κ−PVIIA (Fig. 3 *A*). In the control distributions, the fast shut component was usually ~0.9 ms and corresponded to 80% to 90% of the events, whereas the larger time constant was usually ~6 ms (Fig. 3 *A*, left). As previously found, in the −20- to +40-mV interval, the shut event distributions were not voltage sensitive (Hoshi et al., 1994). In the presence of 1 μM κ-PVIIA, two exponential components were also usually enough to fit the shut distributions; however long shut events became more frequent and longer in duration (Fig. 3 *A*, right). These longer episodes presumably represent blockade events, and a precise analysis of them could produce an estimate of the dissociation rate of the toxin from the open channel. However, because of the relatively low frequency of blocking events, transitions to the slow inactivated state and to the 6-ms shut population would severely contaminate any estimation of the mean blocked time. Instead, my rationale was to focus on the
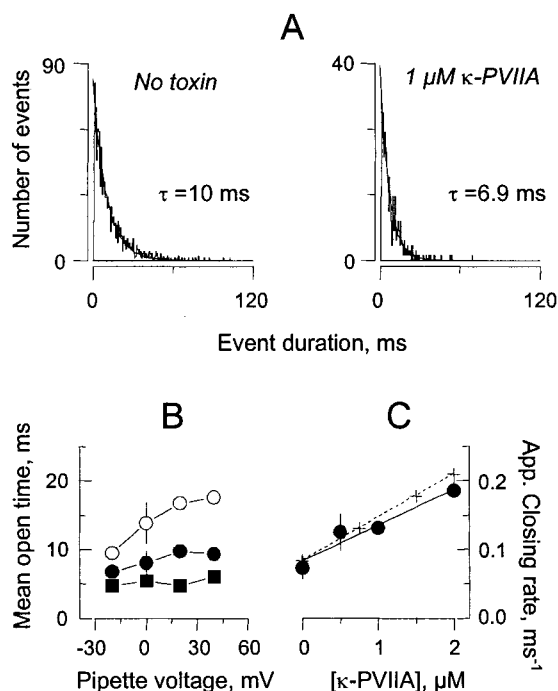
FIGURE 4 κ−PVIIA modifies open time distribution. (*A*) Open time distributions in the absence (*left panel*) and in the presence of 1 μM κ−PVIIA (*right panel*) for the experiment shown in Fig. 2 at 0 mV. Solid lines are single exponential fits to the distributions whose time constants are shown on each panel. (*B*) κ−PVIIA reduces the mean open time in a concentration-dependent manner. Symbols as in Fig. 3 *B*. (*C*) The apparent closing rate increased linearly with the toxin concentration. Plotted experimental data are the average of two to six patches at 0 mV (●), whereas the solid line was draw according to $\tau^{-1} = \beta + k_{\mathrm{ono}}[\kappa$-PVIIA], with $k_{\mathrm{ono}} = 56$ μM^{-1} s^{-1} and $\beta = 83$ s^{-1}. The apparent closing rates for the simulated data arising from scheme I (see Materials and Methods) are plotted as (+). Rate constants for the simulated data were: α and β, were taken as 1100 s^{-1} and 83 s^{-1}, respectively; rates k_{ono} and k_{offo} were 52 μM^{-1} s^{-1} and 25 s^{-1}, respectively (García et al., 1999; and k_{onc} and k_{offc} were 22 μM^{-1} s^{-1} and 1 s^{-1} (Terlau et al., 1999).

latency to the first opening as an estimate of the toxin's dissociation rate. Because the inhibition constant of the κ-PVIIA for the resting channels is 50 to 60 nM, a large percentage (~95%) of the single channel traces should begin with channels already blocked when 1 μM of the toxin is present (García et al., 1999; Terlau et al., 1999). Because κ-PVIIA does not interfere importantly with the much faster gating kinetics of the blocked *Shaker* K channels (García et al., 1999), the first latency would closely represent toxin unbinding events.

Fig. 3 *B* compares the cumulative distribution of the first latency for the membrane patch shown in Fig. 2 in the absence (thin traces) and in the presence of 1 μM κ−PVIIA (thick traces) at 0 mV (left) and +40 mV (right). At all studied voltages the first latency got significantly longer with κ−PVIIA, and it was shorter for more positive voltages (compare thick traces at 0 and +40 mV). Fig. 3 *C* plots the first latency as a function of the voltage for 0, 0.5, and

2 μM κ−PVIIA (in open circles, filled circles, and filled squares, respectively). At all explored voltages, with κ−PVIIA the first opening appeared with approximately 10-fold longer delay. At either 0.5 or 2 μM toxin, the first latencies were fairly similar, suggesting concentration independence. Such suggestion is also exemplified in Fig. 3 *D*, which shows that the average time to first opening at 0 mV was independent of the toxin concentration. Thus, the first latency is concentration independent and voltage dependent. Then, the reciprocal of the first latency may be a good estimate of the dissociation rate of κ−PVIIA from open *Shaker* K channels. Such agreement is summarized in Table 1.

Open time distributions and the association rate constant

Control open time distributions were fitted well with single exponential functions, in agreement with previous reports (Fig. 4 *A* left; see Hoshi et al. 1994). The modification introduced by κ-PVIIA was a decrease of the apparent mean open time without adding new components to the distributions (Fig. 4 *A* right). Such a decrease was seen at every studied voltage and became more pronounced as the toxin concentration was elevated (Fig. 4 *B*). The apparent closing rate was a linear function of κ-PVIIA concentration and Fig. 4 *C* summarizes this observation for 0 mV. Such reduction is naturally expected from scheme I in Materials and Methods. The apparent closing rate depends linearly on the toxin concentration as: $\tau^{-1} = \beta + k_{\mathrm{ono}}[\kappa$-PVIIA], with k_{ono} as the slope and the closing rate, β, as the intercept. The solid line in Fig. 4 *C* was drawn assuming $k_{\mathrm{ono}} = 52$ s^{-1} μM^{-1} and $\beta = 83$ s^{-1}. A summary of such an analysis, done at different voltages, is shown in Table 1. Agreeing with macroscopic estimations, a shallow voltage dependency for the association rate was found.

Simulations of single channel records arising from the simplistic scheme I were performed to test this interpretation (see Materials and Methods). Opening and closing rates for the toxin-free channel, α and β, were taken as 1100 s^{-1} and 83 s^{-1}, respectively. Such values were obtained from the open duration distributions and the most prominent component of the shut duration distributions at 0 mV (Figs. 3 *A* and 4 *A*). Association and dissociation rates for open channels and closed channels were taken from previous macroscopic measurements. For the open state, k_{ono} and k_{offo} were taken from García et al. (1999), and for closed channels, k_{onc} and k_{offc} were taken from Terlau et al. (1999). Microscopic reversibility was assumed to calculate the ratio between the closing and opening rates in blocked channels, y/x. In agreement with the experimental data, the simulated open time histograms were well fitted by single exponential functions. Simulations also accounted for the modification of the apparent closing rate by κ−PVIIA (crosses in Fig. 4 *C*). Thus, with rate constants obtained from previous mac-
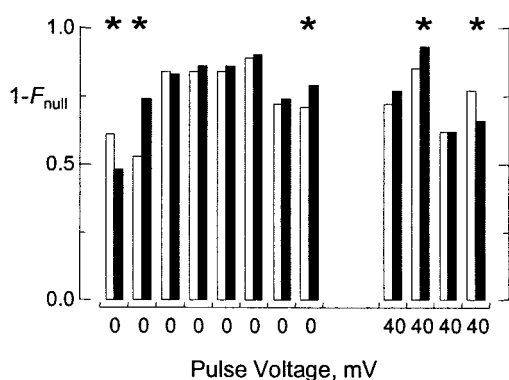
FIGURE 5 κ−PVIIA does not modify the proportion of null traces. The fraction of nonnull traces with or without toxin was computed for experiments having 120 or more traces in the absence and presence of toxin at a given voltage. Shown are the comparisons for 0 and +40 mV. The asterisks indicate comparisons that resulted significantly different in a 2 × 2 contingency table having as a null hypothesis that the toxin does not modify the fraction of null traces ($χ^2 < 3.84$, the significance level of 0.05). Because between 0.5 and 2 $μ$M, occupancy of the resting channels by κ−PVIIA goes from ~0.90 to ~0.97, toxin concentration was disregarded as a variable, and only its presence or absence was considered in this analysis. Each comparison had 140 to 480 control traces, and 120 to 540 toxin traces, making totals of 2510 and 3680 control and toxin traces, respectively.

roscopic studies, the single channel behavior in the presence of κ−PVIIA can be predicted by scheme I.

κ−PVIIA does not affect the proportion of null traces

Nulls, traces without any opening, provide an estimation of the fraction of the time a channel was residing in the slow, presumably, C-inactivated state (Hoshi et al., 1991). They are interpreted as instances when the *Shaker* K channel in the patch goes undetected to the inactivated state; or never opens, because it was already inactivated before the activating voltage pulse (Horn et al., 1981; Marom and Levitan, 1994). Slow inactivation is proposed to imply a constriction of the external mouth of the pore that presumably involves, among others, residues F425, M448, and T449 (López-Barneo et al., 1993: Liu et al., 1996; Molina et al., 1998; Pérez-Cornejo, 1999). These residues are also important for κ−PVIIA binding (Scanlon et al., 1997; Shon et al., 1998; Jacobsen et al., 2000). Then, a comparison of the null traces in the presence and absence of the toxin seemed warranted. Although that the toxin significantly increased the latency to the first opening, the overall fraction of null traces remained unchanged (see for example Figs. 2 and 3 *B*). A more complete study, documenting this lack of effect on the proportion of nulls is summarized in Fig. 5. Because κ−PVIIA occupancy of resting *Shaker* K channels was always 0.9 or higher, only toxin presence or absence was considered in this analysis. The proportions of nonnull

traces with toxin and their respective controls (filled bars and open bars, respectively) are plotted for 12 patches having a large number of traces in each test condition (see legend to Fig. 5 for details). Two voltage pulses, 0 mV and +40 mV, having the largest data sets were chosen to illustrate the toxin effect on the null traces. The proportions of null traces were nearly identical for most of the comparisons. In 7 of the 12 cases shown, the null hypothesis (that the toxin did not modify the fraction of nonnull traces) could not be rejected with a significance level of 0.05. However, for resting five significantly different comparisons (marked with asterisk on top of the bars) there is no obvious tendency for a possible toxin effect on the proportion of null traces. Similar results were also observed at −20 and +20 mV (not shown).

The apparent lack of interaction with the slow inactivation harmonizes with the observation of Fig. 1 in which κ−PVIIA does not appear to modify the macroscopic rate of slow inactivation. Also, it is in agreement with that the bindings of AgTx II to closed or slow inactivated *Shaker* K channels are indistinguishable (Liu et al., 1996).

DISCUSSION

Early work based on macroscopic measurements proposed that κ−PVIIA occludes the pore of K channels. This conclusion was mostly based in two different observations. First, the voltage-dependency and the absolute rate of the toxin unbinding is largely reduced when the internal potassium ions are completely replaced by nonpermeant cations (García et al., 1999). Second, pore flanking residues, F425, T449 are important for the toxin binding (Scanlon et al., 1997; Shon et al., 1998; Jacobsen et al., 2000). Thus, the proposed mechanism is analogous to that of scorpion toxins of the family of α−KTX (MacKinnon and Miller, 1988; Goldstein and Miller, 1993).

Rate constants

The magnitudes of the association and dissociation rate constants appearing here are consistent with scheme I and agree to those obtained form macroscopic studies. The toxin-induced reduction of the mean open time appears to provide a straightforward interpretation for the association rate according to scheme I. However, the first latency analysis to assess the dissociation kinetics requires a bit more justification. The experimental strategy used here was based on the fact that κ−PVIIA binds with ~10-fold higher affinity to the resting than to the open channels. When the blocked resting channels are forced to open by the voltage pulse, they appear to gate conventionally. This is supported by the fact that the macroscopic time constants and the steady-state inhibition observed when the toxin is applied to already-open channels are indistinguishable from those seen

when the channels are opened in the presence of the toxin (García et al., 1999). Thus, the first latency in the presence of κ−PVIIA probably represents an unbinding episode instead of an opening event. In this context, the reciprocal of the first latency is a reasonable estimate of the dissociation rate; it has the proper voltage-dependence and is concentration independent (Fig. 3). However, we have to keep in mind that the analysis of the shut time distributions provides a more rigorous determination of this rate. That analysis requires a larger set of data to distinguish the blocked-events population from longer closures and slow inactivated events (Fig. 3 *A*).

Slow inactivation and toxin binding

In addition to the fast N-inactivation gating that works on the order of few milliseconds range, *Shaker* K channels are endowed with a usually slower inactivation process, in the hundreds of milliseconds range (Hoshi et al., 1991). This process probably involves a constriction of the potassium permeation pathway promoted by a concerted rearrangement of residues flanking the external entrance of the pore (for example, see Yellen et al., 1994; Liu et al., 1996; Ortega-Sáenz et al., 2000; Panyi et al., 1995; Ogielska et al., 1995; Larsson and Elinder, 2000). At least three residues involved in such reorientation are also important for κ−PVIIA binding; 425, 448, and 449 (López-Barneo et al., 1993; Liu et al., 1996; Pérez-Cornejo, 1999; Scanlon et al., 1997; Shon et al., 1998; Jacobsen et al., 2000). The apparent lack of effects of κ−PVIIA on the macroscopic inactivation (Fig. 1), and on the proportion of null traces (Figs. 3 and 5), suggests that the toxin binds equally well to inactivated and noninactivated channels. Analogously, AgTx II, a well-known pore-occluding α−KTx scorpion toxin, binds equally well to either closed or C-inactivated channels (Liu et al., 1996). As for κ−PVIIA, residues 425, 448, and 449 are also important for AgTxII binding to *Shaker* vestibule (Gross and MacKinnon, 1996; Ranganathan et al., 1996). Thus, although we cannot be certain that the null traces are due exclusively to visits to the slow inactivated state, the lack of an interaction of this pore-occluding toxin with the slow inactivation gate falls within a more general scheme.

How large is the protein rearrangement leading to the slow inactivated state that does not affect toxin binding? Cysteine substitution experiments provide some hints on this issue. Cd^{2+} bind with a rate 45,000 faster to slow inactivated T449C channels (Yellen et al., 1994). At positions 448, 449, and 450, Liu et al. (1996) measured in the slow inactivated channel increments of ~100, ~1000, and a ~10,000-fold in the rate of cysteine modification by methanethiosulfonate derivatives, respectively. The rates approached 10,000 to 50,000 μM^{-1} s^{-1}, close to sulfhydryl modification rates in solution (Stauffer and Karlin, 1994). These results suggest large changes in the solvent exposed surface of the cysteine residues during slow inactivation. In

1996, Liu and co-workers suggested a very localized mouth rearrangement for the slow inactivated state. However, taking the Kcsa K-channel as structural template (Doyle et al., 1998; Ranganathan et al., 1996), these residue rearrangements span a substantial 20% to 30% of the toxin-receptor area. This is a significant amount to not be noticed by the toxin. Additionally, the changes in exposure of the residues studied by Liu et al. (1996) were larger for those whose β−carbons are located more distant from the pore in the crystal structure, as if these residues moved more. A possible, although speculative, explanation for a lack of an effect on toxin binding would imply a rearrangement in which the relative positions of at least 425, 448, and 449 do not change drastically. Because at least two, and possibly four, 449 residues simultaneously touch α−KTx scorpion toxins (Naranjo and Miller, 1996; Gross and MacKinnon, 1996), a geometrical constraint must be imposed on such a rearrangement. This constraint would be satisfied by a concerted planar rotation of the vestibule around the pore, as it has been recently proposed for the Pore-S6 loop (Larsson and Elinder, 2000). This simple rotational movement of the vestibule would twist the pore linings. Twisting movement of pore linings are common in ion channel gates (for example, the gap-junction hemichannel, the nicotinic acetylcholine receptor, and the KcsA K-channel) (Unwin and Zampighi, 1980; Unwin, 1995; Perozo et al., 1999). Following Molina et al. (1998), this proposal could explain why when aromatic residues are present in position 449, TEA blocks in nearly voltage independent fashion and does not interfere with the slow inactivation. But, in the wild-type 449T-*Shaker*, TEA blockade is voltage dependent and interferes competitively with the slow inactivation gate, as if TEA was going deeper into the pore. However, a note of caution to this explanation arises from recent theoretical calculations that position TEA closer to the pore when aromatic residues substitute for threonine at position 449 (Crouzy et al., 2001).

REFERENCES

Alvarez, O., A. Villarroel, and G. Eisenman. 1992. Calculation of ion currents from energy profiles and energy profiles from ion currents in multibarrier, multisite, multioccupancy channel models. *Methods Enzymol.* 207:816–854.

Bontems, F., B. Gilquin, C. Roumestand, A. Menez, and F. Toma. 1992. Analysis of side-chain organization on a refined model of

charybdotoxin: structural and functional implications. *Biochemistry.* 31: 7756−7764.

Colquhoun, D., and F. J. Sigworth. 1983. Fitting and statistical analysis of single-channel records. *In* Single Channel Recording. B. Sakmann and E. Neher, editors. Plenum Press, New York. 191−263.

Crouzy, S., S. Bernèche, and Benoît Roux. 2001. Extracellular blockade of K$^+$ channels by TEA: results from molecular dynamics simulations of the KcsA channel. *J. Gen. Physiol.* 118:207−218.

Dauplais, M., A. Lecoq, J. Song, J. Cotton, N. Jamin, B. Gilquin, C. Roumestand, C. Vita, C. L. C. de Medeiros, E. G. Rowan, A. L. Harvey, and A. Ménez. 1997. On the convergent evolution of animal toxins conservation of a diad of functional residues in potassium channel-blocking toxins with unrelated structures. *J. Biol. Chem.* 272: 4302−4309.

DeFelice, L., and J. Clay. 1983. Membrane current and membrane potential form single-channel kinetics. *In* Single Channel Recording. B. Sakmann and E. Neher, editors. Plenum Press, New York. 323−342.

Doyle, D. A., J. Morais-Cabral, R. A. Pfuetzner, A. Kuo, J. M. Gulbis, S. L. Cohen, B. T. Chait, and R. MacKinnon. 1998. The structure of the potassium channel: molecular basis of K$+$ conduction and selectivity. *Science.* 280:69−77.

García, E., M. Scanlon, and D. Naranjo. 1999. A marine snail neurotoxin shares with scorpion toxins a convergent mechanism of blockade on the pore of voltage gated K channels. *J. Gen. Physiol.* 114:141−157.

Goldstein, S. A. N., and C. Miller. 1993. Mechanism of charybdotoxin block of a voltage-gated K$^+$ channel. *Biophys. J.* 5:1613−1619.

Goldstein, S. A. N., D. J. Pheasant, and C. Miller. 1994. The charybdotoxin receptor of a *Shaker* K$^+$ channel: peptide and channel residues mediating molecular recognition. *Neuron.* 12:1377−1388.

Gross, A., and R. MacKinnon. 1996. Agitoxin footprinting the *Shaker* potassium channel pore. *Neuron.* 16:399−406.

Horn, R., J. Patlak, and C. F. Stevens. 1981. Sodium channels need not open before they inactivate. *Nature.* 291:426−427.

Hoshi, T., W. N. Zagotta, and R. W. Aldrich. 1990. Biophysical and molecular mechanisms of *Shaker* potassium channel inactivation. *Science.* 250:533−538.

Hoshi, T., W. N. Zagotta, and R. W. Aldrich. 1991. Two types of inactivation in *Shaker* K$+$ channels: effects of alterations in the carboxy-terminal region. *Neuron.* 7:547−556.

Hoshi, T., W. N. Zagotta, and R. W. Aldrich. 1994. *Shaker* potassium channel gating I: transitions near the open state. *J. Gen. Physiol.* 103: 249−278.

Imredy, J. P., and R. MacKinnon. 2000. Energetic and structural interactions between delta-dendrotoxin and a voltage-gated potassium channel. *J. Mol. Biol.* 296:1283−1294.

Jacobsen, R. B., E. D. Koch, B. Lange-Malecki, M. Stocker, J. Verhey, R. M. Van Wagoner, A. Vyazovkina, B. M. Olivera, and H. Terlau. 2000. Single amino acid substitutions in κ−conotoxin PVIIA disrupt interaction with the *Shaker* K$+$ channel. *J. Biol. Chem.* 275: 24639−24644.

Larsson, H. P., and F. Elinder. 2000. A conserved glutamate is important for slow inactivation in K$+$ channels. *Neuron.* 27:573−583.

Liu, Y., M. Jurman, and G. Yellen. 1996. Dynamic rearrangement of the outer mouth of a potassium channel during gating. *Neuron.* 16:859−867.

López-Barneo, J., T. Hoshi, S. Heinemann, and R. W. Aldrich. 1993. Effects of external cations and mutations in the pore region on C-type inactivation of Shaker potassium channels. *Receptor Channels.* 1:61−71.

MacKinnon, R., and C. Miller. 1988. Mechanism of charybdotoxin block of Ca^{2+}-activated K$+$ channels. *J. Gen. Physiol.* 91:335−349.

Marom, S., and I. B. Levitan. 1994. State-dependent inactivation of the Kv3 potassium channel. *Biophys. J.* 67:579−589.

Molina, A., P. Ortega-Sáenz, and J. López-Barneo. 1998. Pore mutations alter closing and opening kinetics in *Shaker* K$+$channels. *J. Physiol.* 509:327−337.

Naranjo, D., and P. Brehm. 1993. Modal shifts in acetylcholine receptor channel gating confer subunit-dependent desensitization. *Science.* 260: 1811−1814.

Naranjo, D., and C. Miller. 1996. A strongly interacting pair of residues on the contact surface of charybdotoxin and a *Shaker* K$+$ channel. *Neuron.* 16:123−130.

Ogielska, E. M., W. N. Zagotta, T. Hoshi, S. H. Heinemann, J. Haab, and R. W. Aldrich. 1995. Cooperative subunit interactions in C-type inactivation of K channels. *Biophys. J.* 69:2449−2457.

Ortega-Sáenz, P., R. Pardal, A. Castellano, and J. López-Barneo. 2000. Collapse of conductance is prevented by a glutamate residue conserved in voltage-dependent K$^+$ channels. *J. Gen. Physiol.* 116:181−190.

Panyi, G., Z. Sheng, and C. Deutsch. 1995. C-type inactivation of a voltage-gated K$+$ channel occurs by a cooperative mechanism. *Biophys. J.* 69:896−903.

Park, C. S., and C. Miller. 1992. Interaction of charybdotoxin with permeant ions inside the pore of a K$^+$ channel. *Neuron.* 9:307−313.

Pérez-Cornejo, P. 1999. H$+$ ion modulation of C-type inactivation of *Shaker* K$+$ channels. *Pflugers Arch.* 437:865−870.

Perozo, E., D. M. Cortes, and L. G. Cuello. 1999. Structural rearrangements underlying K$+$-channel activation gating. *Science.* 285:73−78.

Ranganathan. R., J. H. Lewis, and R. MacKinnon. 1996. Spatial localization of the K$+$ channel selectivity filter by mutant cycle-based structure analysis. *Neuron.* 16:131−139.

Savarin, P., M. Guenneugues, B. Gilquin, H. Lamthanh, S. Gasparini, S. Zinn-Justin, and A. Ménez. 1998. Three-dimensional structure of κ-conotoxin PVIIA, a novel potassium channel-blocking toxin from cone snails. *Biochemistry.* 37:5407−5416.

Scanlon, M., D. Naranjo, L. Thomas, P. Alewood, R. Lewis, and D. Craik. 1997. Solution structure and proposed binding mechanism of a novel potassium channel toxin κ-conotoxin PVIIA. *Structure.* 5:1585−1597.

Shon, K-J., M. Stocker, H. Terlau, W. Stühmer, R. Jacobsen, C. Walker, M. Grilley, M. Watkins, D. R. Hillyard, W. R. Gray, and B. M. Olivera. 1998. κ-contoxin pviia is a peptide inhibiting the *Shaker* K-channel. *J. Biol. Chem.* 273:33−38.

Stampe, P., L. Kolmakova-Partensky, and C. Miller. 1994. Intimations of K$^+$ channel structure from a complete functional map of the molecular surface of charybdotoxin. *Biochemistry.* 33:443−450.

Stauffer, D. A., and A. Karlin. 1994. Electrostatic potential of the acetylcholine binding sites in the nicotinic receptor probed by reactions of binding-site cysteines with charged methanethiosulfonates. *Biochemistry.* 33:6840−6849.

Terlau, H., A. Boccaccio, B. M. Olivera, and F. Conti. 1999. The block of *Shaker* K$^+$ channels by κ−conotoxin PVIIA is state dependent. *J. Gen. Physiol.* 114:125−140.

Unwin, N. 1995. Acetylcholine receptor channel imaged in the open state. *Nature.* 373:37−43.

Unwin, N., and G. Zampighi. 1980. Structure of the junction between communicating cells. *Nature.* 283:545−549.

Yellen, G., D. Sodickson, T. Y. Chen, and M. E. Jurman. 1994. An engineered cysteine in the external mouth of a K$+$ channel allows inactivation to be modulated by metal binding. *Biophys. J.* 66: 1068−1075.